frontiers | Frontiers in Fuels

TYPE Original Research
PUBLISHED 04 March 2025
DOI 10.3389/ffuel.2025.1528451

OPEN ACCESS

EDITED BY
Foster Agblevor,
Utah State University, United States

REVIEWED BY
Seung-Soo Kim,
Kangwon National University, Republic of Korea
Sandro Barbosa,
Federal University of the Valleys of Jequitinhonha and Mucuri, Brazil

*CORRESPONDENCE
Abul Kalam Hossain,
a.k.hossain@aston.ac.uk

RECEIVED 14 November 2024
ACCEPTED 14 January 2025
PUBLISHED 04 March 2025

CITATION
Masera K, Hossain AK and Griffiths G (2025) Achieving biodiesel standards through saturation level optimisation.
Front. Fuels. 3:1528451.
doi: 10.3389/ffuel.2025.1528451

Achieving biodiesel standards through saturation level optimisation

Kemal Masera[1,2], Abul Kalam Hossain[2]* and Gareth Griffiths[3]

[1]Mechanical Engineering, Middle East Technical University, Kalkanli, Türkiye, [2]Department of Mechanical, Biomedical and Design Engineering, College of Engineering and Physical Sciences, Aston University, Birmingham, United Kingdom, [3]Chemical Engineering and Applied Chemistry, College of Engineering and Physical Sciences, Aston University, Birmingham, United Kingdom

Biodiesels made from waste feedstock are viable sustainable fuels for compression-ignition engine use. However, biodiesels produced from single waste sources do not always comply with the European biodiesel standard. This study investigates fuel quality and engine performance when two biodiesels with different characteristics are blended at various proportions. Waste cooking oil biodiesel was blended with sheep fat biodiesel, which has a lower unsaturated fatty acid content. The engine performance, combustion, and exhaust emission characteristics of the neat biodiesels and their blends (at 60/40, 50/50, and 30/70 ratios) were analysed. The results showed that 60/40 and 50/50 blends met the core parameters of the BS EN 14214 biodiesel standard and improved combustion and emission characteristics compared to neat biodiesels and diesel. The 50/50 blends gave up to 5% and 14% improvements in the in-cylinder pressure and maximum heat release rate, respectively, compared to the same results for neat biodiesel operation. Reduction of up to 73% in CO, 96% in smoke and 3% in CO_2 emissions was observed. However, NOx emission was 2.5% higher than diesel. The results reveal that carefully selected biodiesel–biodiesel blending could meet fuel standards, improve engine performance, and reduce exhaust emissions.

KEYWORDS

biodiesel, biodiesel standards, combustion, emissions, iodine value, saturation level

1 Introduction

Energy consumption continues to increase due to increasing population, technological advancements, and high standards of living, (The World Bank, 2017). According to the World Bank, fossil fuels are the main source of primary energy consumption, with 80% of the market share in 2017 (The World Bank, 2017). The use of conventional fossil fuels causes climate change and associated health problems, particularly in high-density urban areas (Borillo et al., 2018). Demands for sustainable and clean energy sources are growing at a very high rate to adopt to climate action plans set by the governments. The International Energy Agency (IEA, 2019)

Abbreviations: BS EN 14214, British fuel standard for transport biodiesel; BSFC, brake-specific fuel consumption; CA, crank angle; CI, compression ignition; DAG, diglyceride; DI, direct injection; DU, degree of unsaturation; EGR, exhaust gas circulation; EN 590, European diesel standard; FAME, fatty acid methyl ester; FFA, free fatty acid; GC-MS, gas chromatography–mass spectrum; HR, heat release; HRR, heat release rate; IV, iodine value; KOH, potassium hydroxide; MAG, monoacylglycerol; PM, particulate matter; TAG, triacylglycerol; TNHQ, tert-butyl-hydroquinone; TLC, thin layer chromatography; ULSD, ultra-low sulphur diesel; WCO, waste cooking oil.

reported that the share of solar photovoltaic, onshore wind, hydropower, offshore wind, and bioenergy used in 2019 are 57%, 25%, 10%, 4%, and 3%, respectively. Many waste resources can be converted into bioenergy; hence, there is significant potential for increasing its current share of 3%, thereby reducing waste disposal as an added societal bonus. Biodiesel is a promising renewable fuel as it is considered carbon-neutral, energy-efficient, and biodegradable (Salamanca et al., 2012; National Center for Biotechnology Information, 2018). In addition, long-term benefits from using biodiesel in diesel engines on parameters such as lower engine wear and reduced engine oil consumption have been reported by Rajkumar and Thangaraja (2019). The mandatory percentage of biodiesel in transport fuel was 7% (B7) in the United Kingdom (UK) in 2019 (European Standard, 2009). This value was set to increase to 10% in 2020, with further increases in biodiesel share in transport fuel expected (Forte et al., 2018; Masera and Hossain, 2019) at least until 2030, when there will be a ban on the sale of pure internal combustion engine cars in the UK.

Waste cooking oils (WCO) and animal fats are the most common feedstock used to produce biodiesel (Hajjari et al., 2017). However, WCO biodiesel frequently fails to meet fuel standards (BS EN 14214), particularly due to its iodine content (Refaat, 2009; Demirbas, 2009). This can be linked to the chemical structure of WCOs with their double bonds between carbons, which reflects the fatty acid composition of plant-based oils. In contrast, animal fats have fewer double bonds between the carbons in their chemical structures, which removes concerns regarding the iodine content but causes another concern over their viscosity—animal-fat biodiesels are likely to have higher viscosities and freezing points than the limits set by the BS EN 14214 standard (Bhatti et al., 2008). The most common applications for increasing the fuel properties of biodiesels are blending with fossil diesel and doping fuel additives like antioxidants and alcohols. Sathyamurthy et al. (2021) studied the engine performance of corn oil biodiesel blended with diesel at volume percentages of 10%, 20%, and 30%. They found that engine efficiency was reduced with the increasing biodiesel fraction in the blend, but the CO emission of the biodiesel blends were reported around 20% lower than fossil diesel. Attia et al. (2020) investigated the influence of the castor oil biodiesel blending ratio on engine test results. They reported the best BSFC and thermal efficiency for the 20% biodiesel and 80% fossil diesel blend, but maximum exhaust gas emission reductions were addressed for the 10% biodiesel and 90% fossil diesel blend. Kumar et al. (2022) and Verma et al. (2020) studied fossil diesel biodiesel blends in the presence of alcohol additives. The former used ethanol with volume fractions of 5%–15% for blending with biodiesel at volume fractions between 20% and 40%, where the rest of the blends were the fossil diesel They reported improvements in the fuel properties of the overall blend in terms of cold filter plugging point and cetane index (Kumar et al., 2022). The latter studied two alcohol additives—ethanol and methanol—for blending with microalgae biodiesel and fossil diesel (Verma et al., 2020). They observed the maximum reductions in exhaust gas emissions of PM, smoke, and soot emissions with the ethanol, diesel, and biodiesel blend but also noted that the same fuel had increased emissions of NO_x and CO_2 compared to the base fuel (Verma et al., 2020). Rajamohan et al. (2022) studied the effect of synthetic antioxidants, including propyl gallate, butylated hydroxy toluene, pyrogallol, and tert-butyl-hydroquinone (TBHQ) on biodiesel's oxidation stability and engine test results. They reported TBHQ as the best antioxidant additive for the 20% *Prosopis juliflora* biodiesel and 80% fossil diesel blend to obtain enhanced oxidation stability, engine performance, and reduced NOx and CO_2 emissions (Rajamohan et al., 2022).

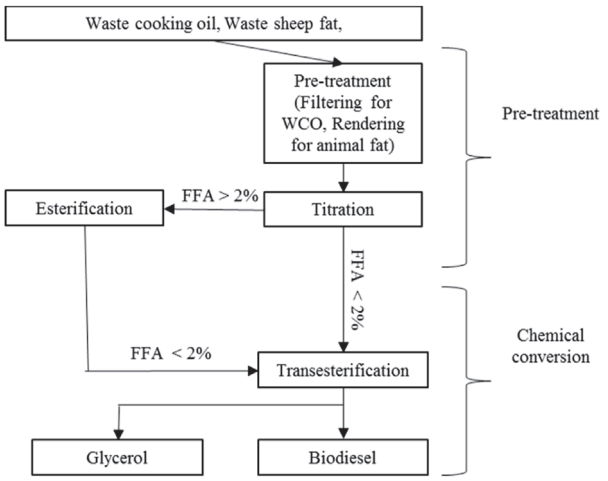

FIGURE 1
Flow diagram of conversion of WCO/animal fats into biodiesel.

Although fossil diesel blending of biodiesel enhances the quality of fuel and reduces exhaust emissions, the technique relies heavily on conventional fossil fuels. Another method for generating high-quality renewable fuel, which complies with the biodiesel fuel standards, is to blend two biodiesels according to their fuel properties—WCO and animal fats. Vegetable oil biodiesels have been blended to reduce economic costs, enhance fuel properties, and aid transesterification (Usta et al., 2005; Sanjid et al., 2016; Sharma and Ganesh, 2019). However, WVO biodiesels are expected to have comparable chemical compositions as they are predominantly composed of unsaturated FAMEs but also contain many polyunsaturated fatty acid breakdown products such as aldehydes and ketones. Animal fat biodiesels, on the other hand, consist of saturated FAMEs and are hence more oxidatively stable; they could be blended with unsaturated biodiesels to obtain upgraded fuel properties, leading to improved engine performance (Masera and Hossain, 2017). Although fossil diesel is used to promote the properties of various biodiesels, there is hardly any study which focuses on biodiesel–biodiesel blending to achieve high fuel quality without using any fossil-based substances. Therefore, the aim of this research is to investigate the blending of WCO biodiesel with a saturated animal fat biodiesel derived from sheep tallow in order to enhance overall fuel properties and combustion characteristics and reduce exhaust gas emissions. The objectives of this study are as follows: (i) producing biodiesels from WCO and animal fats; (ii) blending two biodiesels at various ratios, characterisation of blends, and identifying the optimum blends to match the biodiesel fuel standards; (iii) testing the biodiesel–biodiesel blends in the engine; (iv) assessing the combustion, performance, and emission characteristics of the biodiesel–biodiesel blends; (v) recommending optimum biodiesel–biodiesel blends for diesel engine application. A

10.3389/ffuel.2025.1528451

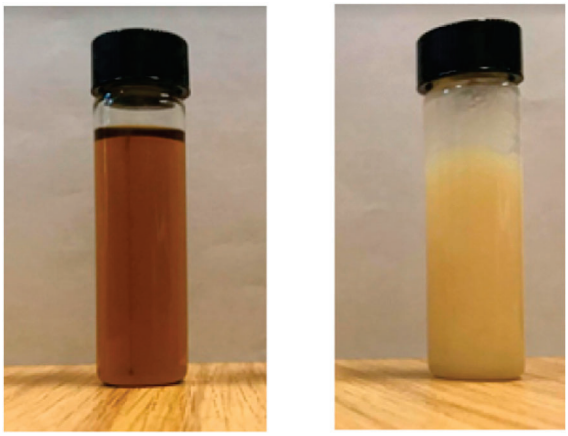

FIGURE 2
Waste cooking oil (left) and sheep fat (right) feedstock after pretreatment.

multi-cylinder, water-cooled compression ignition engine was used for the experiment. Biodiesel production and fuel characterisation were carried out at the Aston University laboratory.

2 Methodology

2.1 Biodiesel production

Two biodiesels from waste sheep fat and WCO were produced to conduct this study. Both feedstock waste fat and WCO were collected from commercially active shops located in Birmingham, UK. Figure 1 shows the biodiesel production flow diagram. To remove any leftover solid particles, a 5-μm sock filter was used to filter the WCO feedstock. The waste fat was rendered at 150°C for 45 min, and the free fatty acid (FFA) content of both WCO and sheep fat was determined by titration (Figure 1). The WCO oil was visibly darker in colour than the sheep fat (Figure 2).

The transesterification reaction was carried out using methanol and KOH as the catalyst. Firstly, the temperature of the feedstock was increased to 65°C, and the solid catalyst was melted in methanol. Secondly, the methanol and KOH solution were transferred to the feedstock at 65°C. Reaction temperature higher than 60°C should be noted as the evaporation temperature of the methanol is approximately 64°C (National Center for Biotechnology Information, 2018). Therefore, a condenser circulating tap water was fitted above the transesterification flask to prevent any methanol evaporating from the system. Magnetic stirrers stirred the mixture for 3 h; the solution was moved to a separator and left for 1 day for the separation of biodiesel and glycerol.

2.2 Fuel characterisation

Fuel properties such as viscosity, density, higher heating value, acid number, flash point, and the carbon, hydrogen, nitrogen, and oxygen contents of various fuel samples were measured according to

TABLE 1 Test engine specifications.

Producer	Lister petter (United Kingdom)
Cylinder capacity	1.395 L
Model	LPWS Bio3
Continuous power at rated speed	9.9 kW
Rated speed	1,500 rpm
Cylinder number	3
Cooling	Water cooled
Aspiration	Naturally aspired
Fuel injection type	Indirect injection
Compression ratio	1:23.5
Exhaust gas recirculation	0%

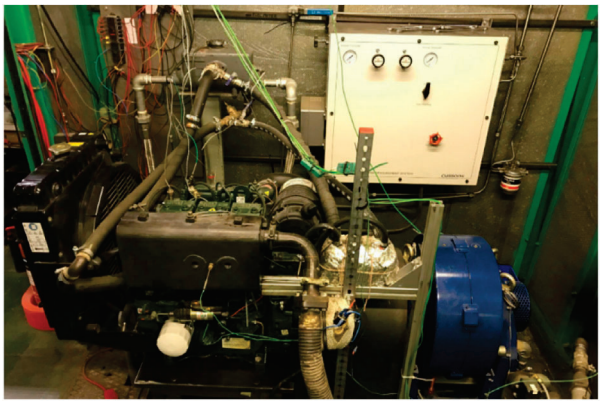

FIGURE 3
Engine test rig coupled with the dynamometer.

British and European standards. The cetane number, lower heating value, iodine value, and degree of unsaturation were calculated from the FAME compositions, which were measured using gas chromatography–mass spectrometry (GC-MS) analysis. Feedstock oils and biodiesel samples were separated into their constituent lipid components using thin layer chromatography (TLC) on Silica gel G using hexane/diethyl ether/acetic acid (70/30/1 v/v/v) as the developing solvent. In the crude oil samples, the major components were triacylglycerol (TAG), free fatty acids (FFA), diacylglycerol (DAG), and monoacylglycerol (MAG). In the case of biodiesel, fatty acid methyl esters (FAMEs) were the major products recovered and analysed. Samples were derivatised to their FAMEs using dry methanol containing 2.5% sulphuric acid by reflux at 70°C for 90 min in hermetically sealed glass Pyrex tubes under nitrogen. The FAMEs were extracted into hexane, partitioned against water, and quantified using heptadecanoic acid as an internal standard on an Agilent Technologies 6890N GC-MS equipped with a DB-23 capillary column (30 m × 0.25 mm and film thickness of 0.25 μm) with helium as the carrier gas. The GC injection was set to split mode at 50:1 ratio, and the inlet temperature was set to 250°C. The temperature at the column was maintained at 50°C for the first

10.3389/ffuel.2025.1528451

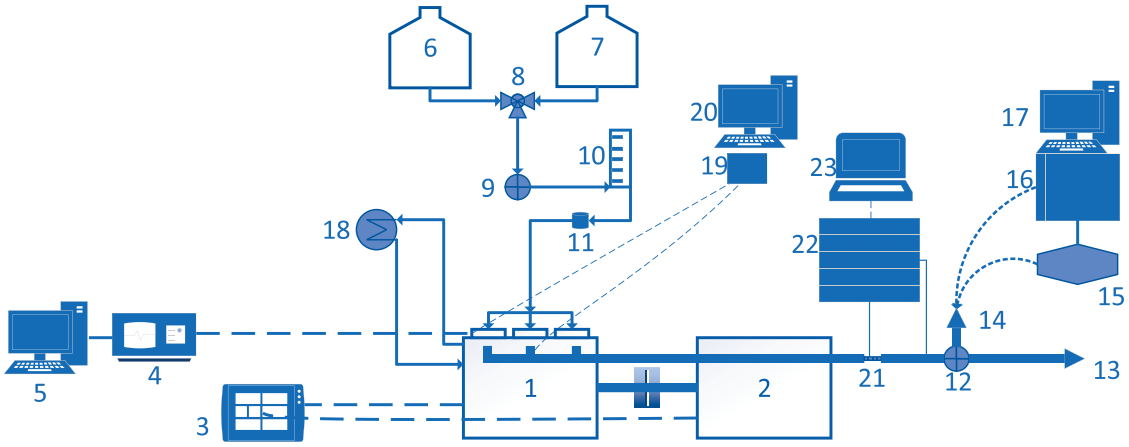

FIGURE 4
Engine test rig schematic of the (1) CI engine, (2) dynamometer, (3) dynamometer controller, (4) Kistler combustion equipment, (5) computer, (6) fossil diesel container, (7) biofuel container, (8) valve, (9) flow controller, (10) fuel flow meter, (11) fuel filter, (12) valve, (13) exhaust outlet, (14) emission measurement station, (15) BOSH smoke measurement unit, (16) exhaust gas analyser, (17) computer, (18) coolant, (19) temperature measurement station, (20) computer, (21) tailpipe attachment for HORIBA emission measurement, (22) HORIBA emission analyser, and (23) laptop.

TABLE 2 Information regarding equipment used in the experiment, adapted from Masera (2019).

Measured parameter	Equipment	Details	Accuracy	Uncertainty (%)
Engine speed	Eddy Current Dynamometer	Froude Hofmann AG80HS	±1 rpm	0.2
Torque	Eddy Current Dynamometer	Froude Hofmann AG80HS	±0.4 Nm	0.8
Time to consume 100 mL of fuel	Scaled cylinder and stopwatch	Manually tested	±0.1 s	0.8
NO	Horiba OBS-ONE-GS02	Heated dual CLD	±1 ppm	0.2
CO	Horiba OBS-ONE-GS02	Heated NDIR	±0.01 vol. %	0.01
NO_x	Horiba OBS-ONE-GS02	Heated dual CLD	±1 ppm	0.2
CO_2	Horiba OBS-ONE-GS02	Heated NDIR	±0.1 vol. %	0.1
Smoke opacity	Bosch	RTM 430	±0.01 m^{-1}	1.4
Exhaust gas temperature	Horiba OBS-ONE-GS02	Tailpipe attachment with pitot	±0.1°C	0.04
In-cylinder pressure	Kistler	6125C11 PS, 5064B11 A	±0.1 bar	0.1
Crank angle	Kistler	An optical encoder, 2614A	±0.1°	0.03
Fuel injection pressure	Kistler	4065A500A0 PS, 4618A0 A	±0.1 bar	0.1
Combustion software	Kistler	KiBoxCockpit		
To log the combustion data	Kistler	2893AK8 model KiBox		

A, amplifier; CLD, chemiluminescence detection; NDIR, non-dispersive infrared detection; PS, pressure sensor.

minute and increased at the rate of 25°C/minute up to 175°C; the second ramp set at a heating rate of 4°C per minute up to 235°C was kept for 15 min. The NIST08 MS library was used to assess the FAMEs.

2.3 Test rig and equipment

A naturally aspired diesel engine with an indirect injection mechanism was used to test the fuels (Table 1). Figure 3 shows the engine mounted to an eddy current type dynamometer.

Figure 4 displays the test rig schematic, including the measurement facilities for engine performance, combustion, and exhaust emission measurements.

The engine was first started with conventional fossil fuel and then warmed up for 30 min to avoid any cold-start effect on the observed results. Test fuel was then fed into the system and allowed to run for a minimum of 15 min to flush the system, and data were then read at the steady-state situation. KiBox equipment was set to observe the characteristics of combustion parameters such as injection start, combustion start, combustion end, in-cylinder pressure, and heat release rate (HRR). An average of 51 cycles

TABLE 3 FAME compositions of the test samples in mass percentages.

FAME	W100	W80A20	W60A40	W50A50	W30A70	W10A90	A100
C14:0	0.1	0.5	0.9	1.2	1.7	2.3	2.8
C16:0	11.0	13.1	14.8	15.8	18.2	20.6	21.6
C16:1	0.0	0.0	0.4	1.0	1.4	1.9	0.9
C18:0	4.0	9.3	14.7	17.9	22.6	27.9	29.3
C18:1	2.6	3.8	5.0	5.9	6.8	7.9	43.5
C18:2	76.8	68.9	60.5	55.0	47.1	38.2	1.1
C18:3	5.4	4.5	3.6	3.1	2.2	1.2	0.8
Saturated	15.1	22.9	30.5	34.9	42.5	50.8	54.4
Monounsaturated	2.6	3.8	5.4	7.0	8.2	9.8	44.4
Polyunsaturated	82.2	73.4	64.1	58.1	49.3	39.4	1.1

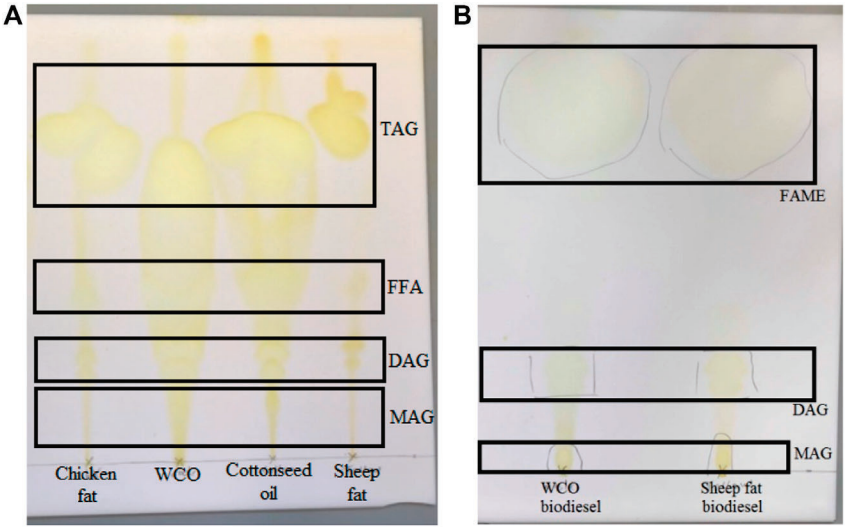

FIGURE 5
Feedstock oils **(A)** and neat biodiesel **(B)**. Samples were tested on thin-layer chromatography (TLC).

was collected and used in the combustion analysis to minimise cycle errors (Awad et al., 2014). CO, CO_2, NO, and NO_x exhaust gases were measured using a Horiba OBS-ONE gas analyser. In addition, Bosch RTM 430 equipment was used to observe the smoke intensity data. Table 2 illustrates the measurement accuracy of the equipment used during the experiment.

2.4 Error analysis

The partial differential method was used to quantify the overall uncertainty of this experimental study (Masera et al., 2021). In the error analysis, the uncertainties of the individual elements given in Table 2 are considered in Equation 1, and the overall uncertainty of the experimental analysis is found to be 1.872%.

$$Uncertainity = \sqrt{\sum (specific\ uncertainties)^2} = \pm 1.872\%. \quad (1)$$

3 Results and discussion

3.1 Fuel characterisation

From 1.8 kg of sheep fat, approximately 1.576 kg of sheep tallow was rendered, yielding an 88% efficiency. The two neat biodiesels were then obtained using transesterification in different containers (Figure 1). These biodiesels were used to develop seven biofuel samples: neat waste cooking oil biodiesel (W100), neat animal fat biodiesel (A100), and their blends at 80–20 (W80A20), 60–40 (W60A40), 50–50 (W50A50), 30–70 (W30A70), and 10–90 (W10A90) volume fractions. In addition to the test samples, a commercial diesel meeting the BS EN 590 standard was purchased from Esso United Kingdom Ltd. and tested to compare the results (Esso, 2019). Table 3 shows the FAME breakdown of the test samples in terms of saturated (C18:0, C16:0, and C14:0), monounsaturated (C18:1 and C16:1), and

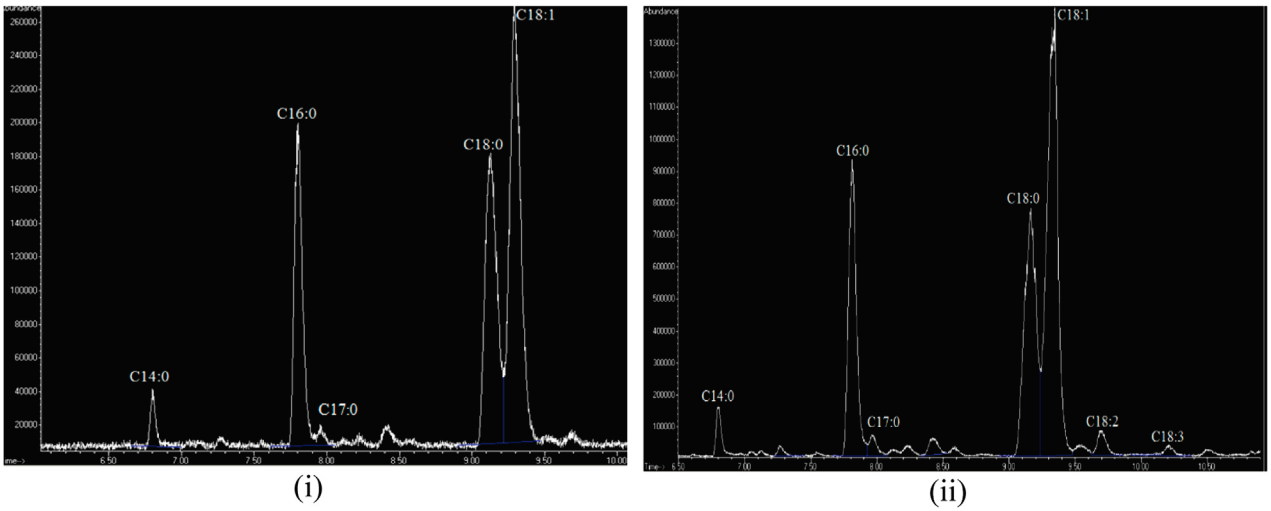

FIGURE 6
Gas chromatography and mass spectrum analysis of waste sheep fat as feedstock TAG (i) and biodiesel FAME (ii) (C17:0 was used as an experimental reference). The A100 predominantly consisted of C16:0 (saturated), C18:0 (saturated), and C18:1 monounsaturated FAMEs.

polyunsaturated (C18:3 and C18:2) FAMEs. W100 mostly consisted of C18:2, whereas this was a minor component in A100. The major components of A100 were C18:1 > 18:0 > 16:0, accounting for ca. 94% of the composition (Table 3). After combining the two neat biodiesels, linear differences in saturated, monounsaturated, and polyunsaturated FAMEs were detected.

Figure 5 shows the TLC chromatogram of WCO, sheep fat, and their biodiesel derivatives. TAGs were the most prevalent (>90%) lipid in the oils, with lower amounts of FFA, DAG, and MAG (Figure 6).

Table 4 illustrates the characteristics of the test samples, reference diesel, BS EN 14214, and EN 590 (British Standard Institution, 2010; Ramírez-Verduzco et al., 2012). According to the results, neither the neat WCO (W100) nor sheep tallow (A100) biodiesels fully met the BS EN 14214 specifications. For example, A100 and biomixtures of W10A90 and W30A70 had viscosities higher than the maximum limit of 5.0 mm^2/s. This can be attributed to the higher presence of saturated FAMEs in their chemical compositions. On the other hand, the W100 and W80A20 biomixture had cetane numbers lower than the minimum limit of 52 as well as iodine values higher than the maximum limit of 120. Similarly, this is due to the higher presence of the unsaturated FAMEs in their chemical structures. However, the fuel properties of the W50A50 and W60A40 biomixtures were found to be within the specified limits in BS EN 14214 specifications in terms of the all test parameters (Masera and Hossain, 2017). This shows that the blending of neat biodiesels can improve the fuel properties by optimising the saturated and unsaturated FAME compositions.

3.2 Combustion characteristics and degree of unsaturation

Figure 7 illustrates (a) combustion start, (b) finish times, and (c) total combustion duration in terms of crank angle position. Figure 7A shows that the test fuels combusted almost at the same crank angle at each engine load. However, combustion end-time increased with respect to increasing engine load (Figure 7B), as the amount of fuel consumed increased to overcome increased resistance. This increase in combustion end time affected the overall combustion duration, which was also increased with respect to increasing engine load (Figure 7C).

A linearly increasing trend was observed for exhaust gas temperature (EGT) with the increasing engine load (Figure 8). The trend was in good agreement with the literature and can be attributed to the increasing amount of fuel needed to overcome the increasing resistance at higher engine loads (Emiroğlu et al., 2018). The combustion of the increased amount of fuel makes the combustion process last longer, which also causes some of the fuel to burn late during the power stroke at larger volumes and puts less pressure on the piston head (Awad et al., 2014). The EGT also had direct impact on the exhaust gas emissions due to the increased tendency of nitrogen and oxygen to react and form NOx at high temperatures (Ragit et al., 2010).

The results given in Figure 9 show that the biofuels have 5–10 bar higher in-cylinder pressure than diesel. This combustion improvement can be linked to the biodiesel's inherent oxygen content. The highest pressure was observed with the W50A50 biomixture, which was approximately 3%–5% higher than neat biodiesels at the high engine loads. Similarly, this can also be associated with the optimised fuel properties of the 50–50 blend, such as medium values of DU and viscosity as 123 and 4.93 mm^2/s.

Figure 10 shows the heat release (HR) of the biofuels and diesel at low, medium, and high engine loads. The negative HR earlier than combustion is deemed due to the fuel evaporation (Bowden et al., 1969). Figure 10I indicates that the HR of the W50A50 and W60A40 blends was approximately 10–20 joules higher than the diesel. During the early combustion phase, the highest HR was recorded for the A100, which was approximately 4% higher than all other test fuels. In contrast, it gave the lowest HR reading at approximately 20 joules lower than to other fuels towards the

TABLE 4 Comparison of test sample fuel characteristics against BS EN 14214 and EN 590 standards (British Standard Institution, 2010; European Standard, 2009).

Fuel properties	Units	Biofuels							Diesel	Standards for	
		W100	W80A20	W60A40	W50A50	W30A70	W10A90	A100		Biodiesel	Diesel
										BS EN 14214	EN 590
Viscosity at 40°C	(mm^2/s)	4.80	4.85	4.90	4.93	5.15	5.33	5.48	2.78	3.5–5.0	2.0–4.5
Density	(g/cm^3)	0.882	0.880	0.874	0.872	0.870	0.868	0.865	0.828	0.86–0.90	0.820–0.845
Flash point	(°C)	169	170	168	168	172	172	170	61.5	min 101	min 55
Cetane number[a]	()	47	50	53	55	58	62	70	53.5	min 51	min 51
Cetane number[b]	()	44	47	51	52	55	58	66	53.5	min 51	min 51
Carbon, theoretical	(%)	77.27	77.16	77.04	76.96	76.84	76.71	76.48	—	—	—
Carbon, measured	(%)	76.56	—	77.48	77.1	75.01	—	76.89	86.6[c]	—	—
Hydrogen, theoretical	(%)	11.74	11.84	11.93	11.99	12.08	12.18	12.43	—	—	—
Hydrogen, measured	(%)	11.86	—	12.12	12.66	12.58	—	12.81	13.4[c]	—	—
Oxygen, theoretical	(%)	10.99	11.01	11.03	11.05	11.08	11.11	11.09	n/a	—	—
Oxygen, measured	(%)	11.58	—	10.41	10.24	12.41	n/a	10.30	0.07[c]	—	—
HHV	(MJ/kg)	38.4	39.8	39.5	39.4	39.2	39.0	40.5	45.16	—	—
LHV	(MJ/kg)	37	37	37	37	37	37	37	42	—	—
Iodine number	(g/100g)	145	130	116	107	92	77	40	—	max 120	—
Linolenic acid methyl ester	(%mol/mol)	5.4	4.5	3.6	3.1	2.2	1.3	0.8	—	max 12	—
Monoacylglycerol (MAG)	(%mol/mol)	N/D	N/D	N/D	N/D	N/D	N/D	N/D	N/D	max 0.8	—
Diglyceride (DAG)	(%mol/mol)	N/D	N/D	N/D	N/D	N/D	N/D	N/D	N/D	max 0.2	—
Triacylglycerol (TAG)	(%mol/mol)	N/D	N/D	N/D	N/D	N/D	N/D	N/D	N/D	max 0.2	—
Methanol	(%mol/mol)	0	0	0	0	0	0	0	—	max 0.2	—
Acid value	(mg KOH/g)	0.200	0.229	0.259	0.289	0.289	0.290	0.291	0.091	max 0.5	—
Degree of unsaturation	(Weight %)	167	150	133	123	107	89	47	—	—	—

[a]Ramírez-Verduzco et al. (2012)
[b]Tong et al. (2011)
[c]Schönborn et al. (2009)
N/D, not detected.

10.3389/ffuel.2025.1528451

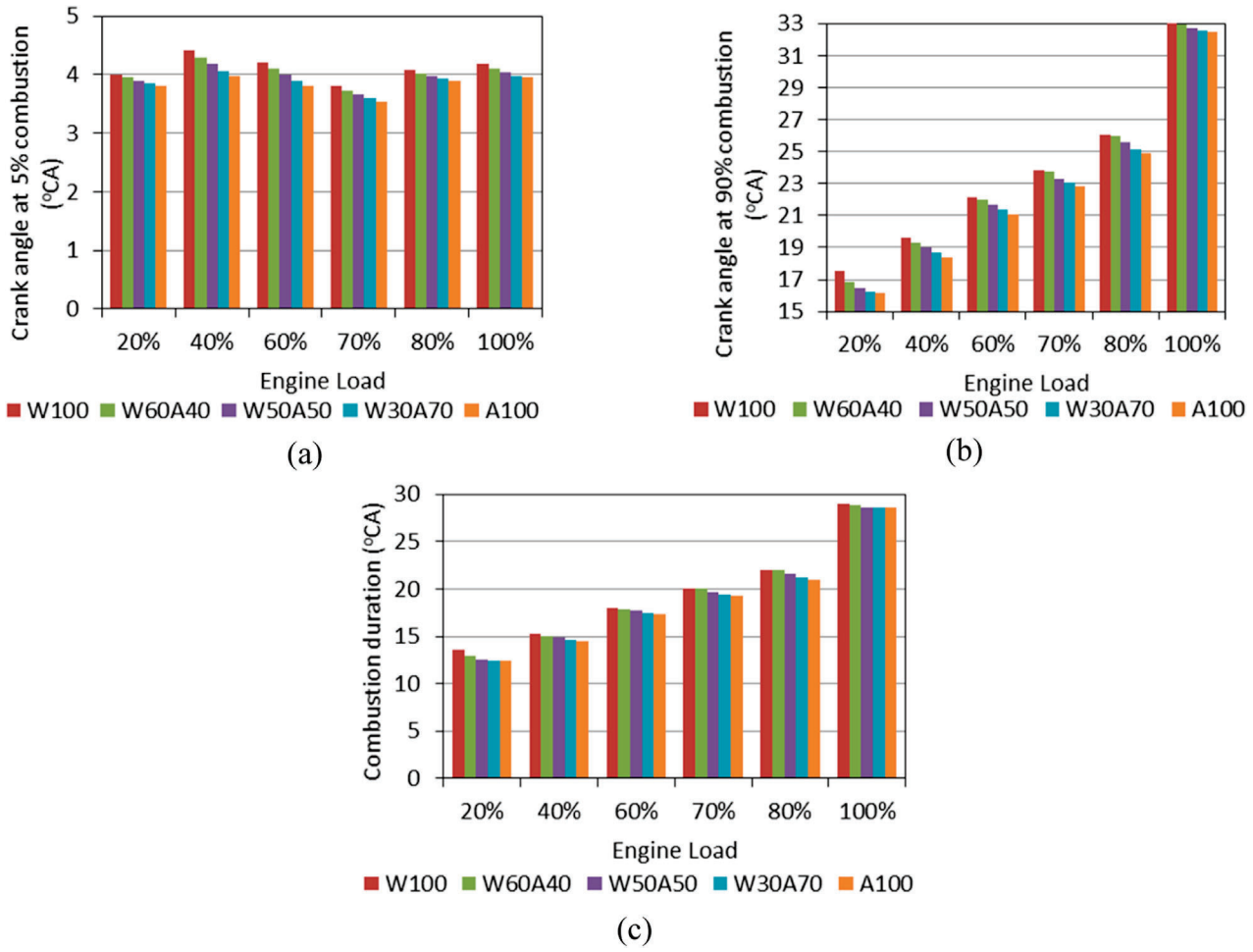

FIGURE 7
Crank angle positions at different stages of combustion: **(A)** beginning, **(B)** end, and **(C)** total combustion duration.

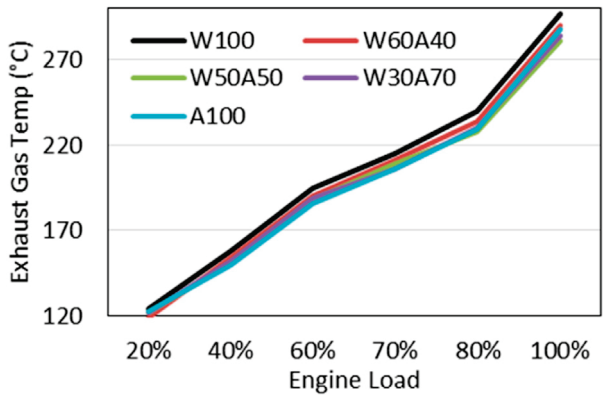

FIGURE 8
Exhaust gas temperatures of biofuels at different engine loads.

combustion end stage—35°CA—whereas the W100 neat biodiesel had the exactly the opposite trend of higher HR towards the end of combustion rather than the early combustion stage. This is deemed due to the increasing unsaturation of the FAMEs, which need higher energy to break the C=C (double) bonds than the C–C (single) bonds in A100 and W30A70, particularly at the initial combustion stage. Consequently, it is understood that the A100 and W100 biodiesels have exactly the opposite combustion characteristics, with the former burning faster and with more HR at the initial combustion stage, whereas the latter has relatively late HR towards the end stages of the combustion. Similar trends were also observed with the A100- and W100-dominated blends.

Figure 11 studies the maximum HRR for the test fuels at various engine loads. According to the results collected at the full engine load, the neat biodiesels and their blends had slightly increased maximum HRR resulting from inherit oxygen content. The lower maximum HRR at the low engine loads can be linked to biodiesel fuel properties such as higher density and viscosity than diesel. The negative effects of these fuel properties were observed especially at low engine loads, where the combustion temperature was also low. Among the biodiesels, the W50A50 blend with the optimised fuel properties provided the highest maximum HRR slightly above 30 J/°CA at the 100% engine load. These results also revealed that the biodiesel fuel property optimisation achieved by blending two neat biodiesels also improved the combustion results of the biomixture compared to neat biodiesels.

10.3389/ffuel.2025.1528451

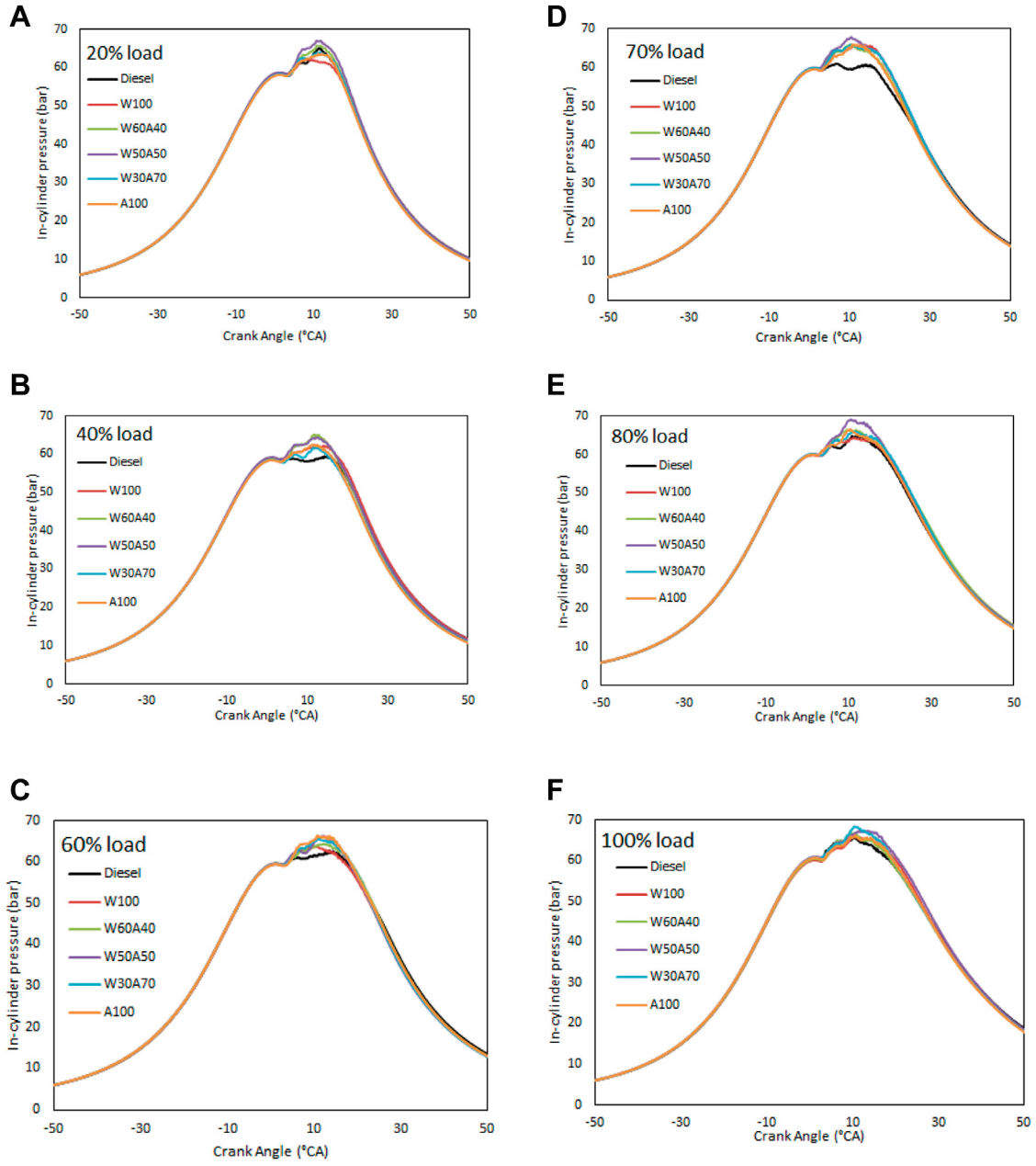

FIGURE 9
In-cylinder pressures of the test fuels at **(A)** 20%, **(B)** 40%, **(C)** 60%, **(D)** 70%, **(E)** 80% and **(F)** 100% engine loads.

3.3 Engine performance

The engine performance parameters of brake-specific energy consumption (BSEC), brake-specific fuel consumption (BSFC), and brake thermal efficiency (BTE) were measured for each test fuel. Figure 12 reveals BSFC values measured at each engine load. The animal fat biodiesel A100 and related biomixtures having high animal fat biodiesel fraction had relatively higher BSFC than other biodiesels at low engine loads due to their high viscosities. However, this disadvantage decreased for the high engine loads. At full load, the average BSFC of biodiesels was approximately 14.5% greater than diesel. The results were consistent with the literature and can be attributed to biodiesel's lower LHV (Özener et al., 2014).

BSEC analysis is suggested for the comparison of fuel with different LHV properties in the literature (Krishna et al., 2016) because it considers not just the amount of fuel utilised but also the LHV property of the fuels. According to Figure 13, the BSEC of the biodiesels and diesel were equivalent, especially at full engine load. Furthermore, at 60% engine load, W50A50, W60A40, and W100 had a BSEC roughly 1.9% lower than diesel. Similarly, at medium engine loads, W100 had the greatest BTE—approximately 8% higher than diesel. Between 20% and 60% engine loads, the W50A50 and W60A40 biomixtures had approximately 2% greater BTE than diesel (Figure 14). The inherit oxygen content of biodiesels is thought to be the primary reason for the enhanced BTE.

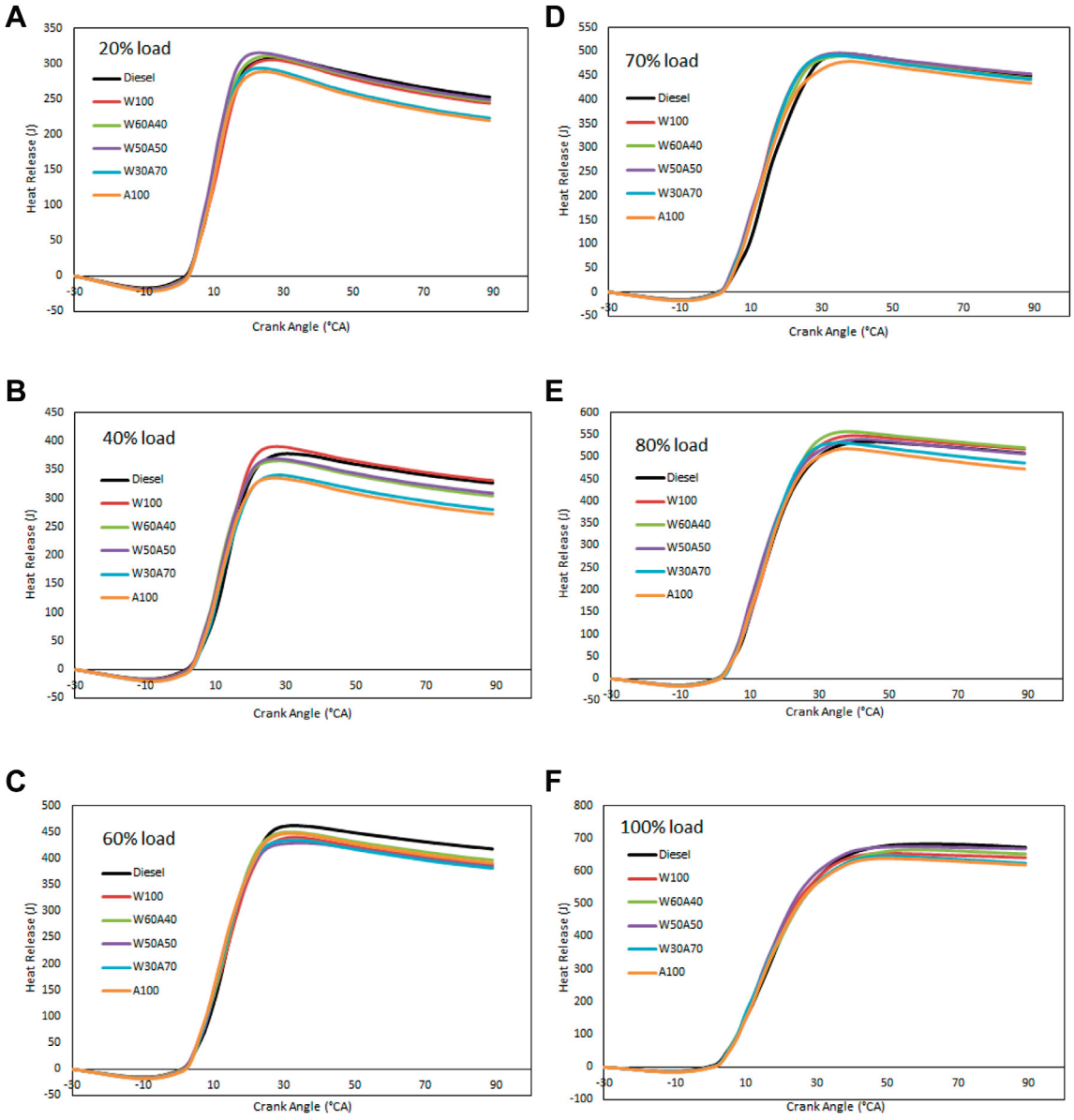

FIGURE 10
Heat release (HR) at **(A)** 20%, **(B)** 40%, **(C)** 60%, **(D)** 70%, **(E)** 80% and **(F)** 100% engine loads.

3.4 Exhaust emissions and degree of unsaturation

The three main elements that influence CO_2 and CO emissions are burning efficiency, oxygen, and carbon contents (Kumar and Subramanian, 2017). Thus, every fuel's CO_2 emissions reveal its combustion efficiency. Acyl carbons react with oxygen molecules and produce CO and CO_2 emissions as a result of combustion. CO is the major product generated under limited O_2 conditions (Wakode and Kanase-Patil, 2017). Figure 15 shows that CO_2 emissions increased linearly with increasing engine loads for all fuels. This can be attributed to the higher fuel consumption as the engine load increases. All biofuels, with the exception of W100, released approximately 6% (15 g/100s at full load) less CO_2 than diesel, on average. Compared to diesel, the W50A50 biomixture reduced CO_2 emissions by 3.6% and 6.7%, respectively. Note that the CO_2 emission of the W100 biodiesel was recorded at 3.1% higher than the diesel, but the rest of the biodiesels—A100, W30A70, W50A50, and W60A40—had 2% to 3% lower CO_2 emissions than diesel at the full engine load.

Figure 16 illustrates CO releases at various engine loads. CO emissions exhibited a similarly increasing trend as CO_2 emissions, which is related to the higher amount of fuel being burned at the higher engine loads. The combustion efficiency of the W100 was found to be the poorest, releasing approximately 0.30 g/100s more CO emissions than other test fuels. Another reason for the higher CO emission was the carbon content of the fuel, which was the greatest amongst the test fuels. The other biodiesel and biomixtures had between 6% and 78% lower CO emission than diesel at 80% engine load. The differences in the fuel properties such as carbon content is one reason for the CO emission variation of the biomixtures (Table 4). The W50A50 biomixture gave

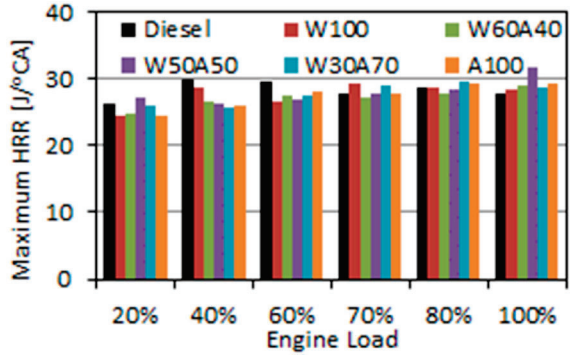

FIGURE 11
Maximum heat release rate (HRR) versus engine load.

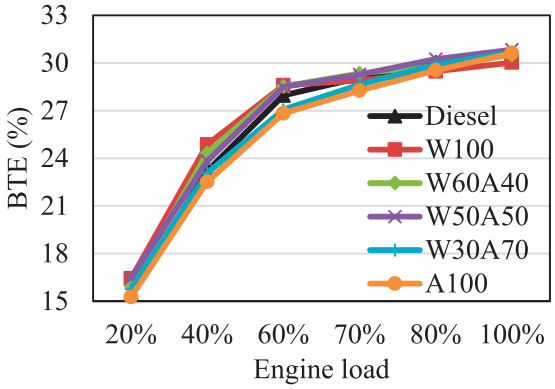

FIGURE 14
Brake thermal efficiency (BTE) at various engine loads.

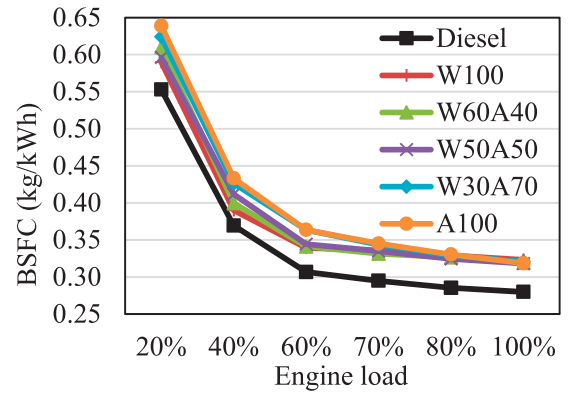

FIGURE 12
Brake-specific fuel consumptions (BSFC) at various engine loads.

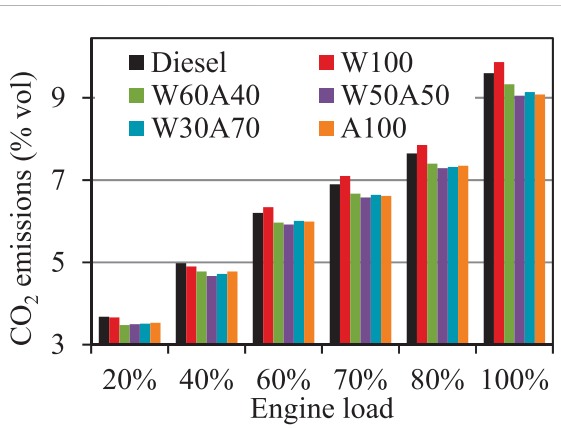

FIGURE 15
CO_2 emissions of test fuels in g/100s.

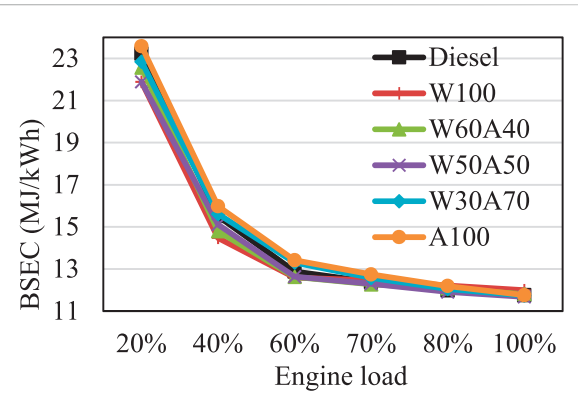

FIGURE 13
Brake-specific energy consumptions (BSEC) at various engine loads.

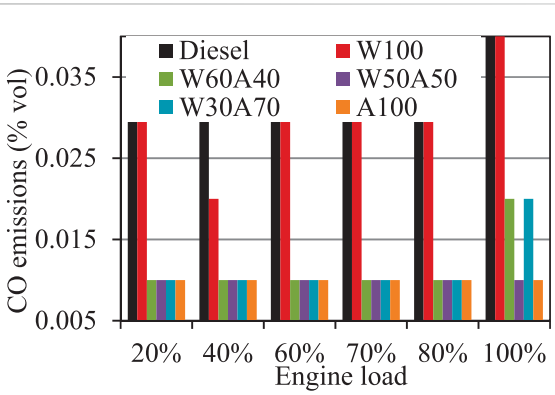

FIGURE 16
CO emissions of the test fuels in g/100s.

the lowest CO gas emission, which was 63%–70% lower than W100 and diesel at 100% engine load.

Figure 17 demonstrates the emission measurements for the NO, NO_2, and NO_x gases at the test loads. The majority of the biodiesels gave higher emissions of NO_x due to the presence of oxygen in their chemical content (e.g., ester bonds in TAG and ester bonds and OH groups in DAG and MAG), which yields higher temperatures during combustion. At full load, the NO and NO_x emissions of all test fuels decreased. The lower oxygen to nitrogen ratio at full load can be attributable to this decreasing trend. For example, A100, W60A40, and W100 respectively emitted approximately 2.9%, 1.2%, and 0.5% less NO emission than diesel at the 100% load. In contrast, W30A70 and

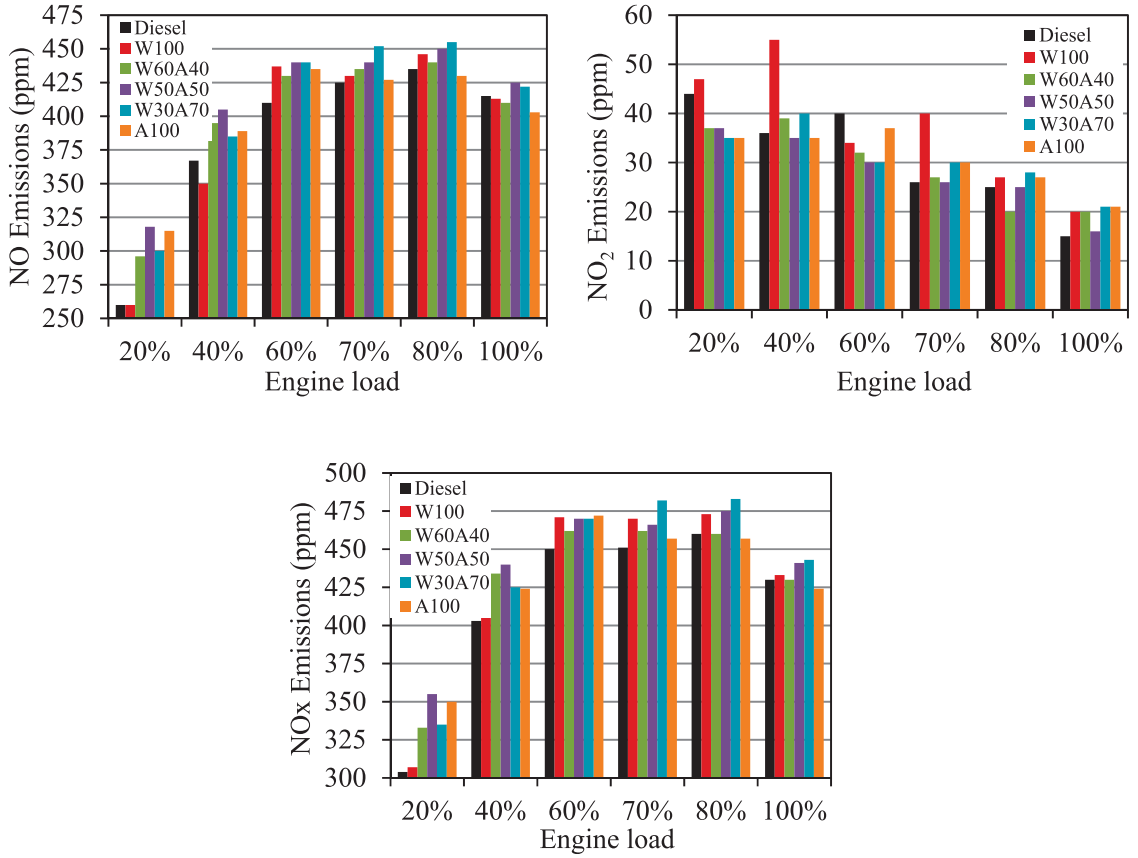

FIGURE 17
NO, NO_2, and NO_x emissions at various engine loads.

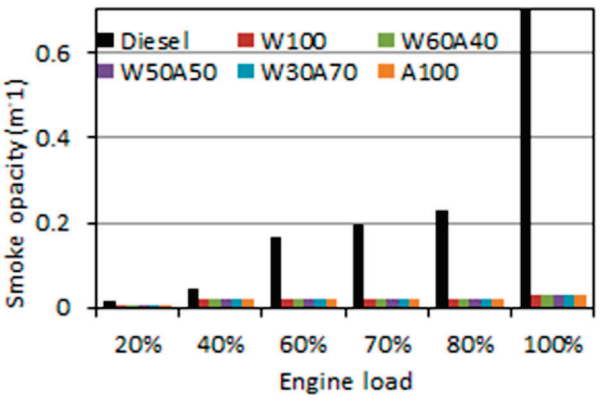

FIGURE 18
Smoke opacity (soot) measurements.

W50A50 emitted 1.7% and 2.4% more NO than diesel. All biodiesels had higher NO_2 emissions than diesel, in the range of 6%–29%. Consequently, the sum of NO and NO_2, which corresponds to NO_x emission, of most biodiesels measured higher than diesel, between 0.7% and 2.9% at the 100% engine load. However, A100 and W60A40 gave comparable NO_x emissions to diesel. Considering the fuel properties meeting the BS EN 14214 standard along with the favourable NOx emission, the W60A40 biomixture can promote the biodiesel–biodiesel blending technique.

Figure 18 illustrates the smoke emissions at each engine load for the test fuels. The results given in Figure 18 show a drastic difference in smoke emission between the biodiesels and diesel, with the maximum reduction of 96% at the 100% engine load. The significantly higher smoke emission of the fossil diesel is deemed due to its content with aromatic hydrocarbons, which are not present in any biodiesel. Their breakdown yields visible smoke, or "soot." The magnitude of the smoke formation increases in the absence of the oxygen, which explains the increasing smoke emission trend of diesel at the higher engine loads (Dhamodaran et al., 2017). Note that as the amount of oxygen intake is kept constant but the amount of fuel is increased with the increasing engine load, the oxygen content gets lower with the increasing engine load. The literature also considers the influences of fuel properties like density, viscosity, and cetane number as well as the combustion behaviour on smoke emission (Dhamodaran et al., 2017; Ragit et al., 2010). However, it is believed that the presence of the aromatic hydrocarbons is the main reason behind the drastic difference. As the smoke emission is visible, the filter of the exhaust gas measurement device was inspected before and after the experiment (Figure 19). The filter given in Figure 19A is used only once to test the diesel, whereas the filter shown in Figure 19B is used to test the five other biodiesels.

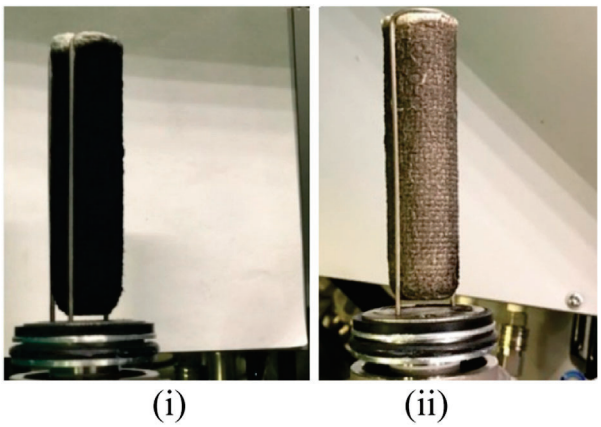

FIGURE 19
Contamination of new equipment filters after testing diesel in one experiment (i) and all test biodiesels, five experiments in total (ii).

4 Conclusion

This study investigated the fuel property optimisation of the two neat biodiesels produced from waste cooking oil (W100) and waste sheep fat (A100) by blending them at various volume fractions. According to fuel characterisation and engine test results, although, the neat biodiesels did not meet the biodiesel standard (BS EN 14214), W50A50 and W60A40 blends complied with it. This can be attributed to the balanced saturation level of the blends, which eliminates the high iodine value and viscosity of neat biodiesels W100 and A100, respectively.

Combustion duration and ignition delay were shortened by 0.5 °CA and 0.05 °CA with each blend's increasing fraction of A100. This shows that the higher cetane number of A100 improved the combustion quality of the blends.

It was also found that the saturation property of a fuel was inversely proportional to the combustion duration, which also affected the exhaust gas temperature. Therefore, the exhaust gas temperatures were increased with the increasing W100 fraction.

The W50A50 fuel had the maximum in-cylinder pressure, which was approximately 3%–5% higher than the neat biodiesels between 10.3 and 12.0 °CA at high engine loads. The improved in-cylinder pressure is linked to saturation level optimisation of the blend, which improved the fuel properties.

The maximum HRR value of W50A50 was respectively 14%, 11%, and 8% greater than diesel, W100, and A100 at 100% load. Although the BTE of the W100 was observed to be approximately 10% greater than diesel, the BSEC and BTC of all test fuels, including diesel, were comparable at 100% engine load.

The W50A50 biomixture gave the lowest CO_2 emission, 3.3% and 6.4% lower than the diesel and neat biodiesel at the 100% engine load condition. In addition, the CO emission of the neat biodiesels and biomixtures was significantly less than diesel at 73%–78% at the 70% engine load condition.

The NO_x emission of the neat biodiesels and the majority of the biomixtures were slightly higher than diesel, with the maximum increase of roughly 3% with W30A70 biomixture at the 100% engine load. However, the NO_x emissions of the W60A40 biomixture and sheep fat biodiesel A100 were comparable to diesel. This can be attributed to the highly saturated content of the A100 biodiesel, which provided a relatively shorter combustion duration and lower combustion temperature.

In summary, this study recommends the blending of two WCO and sheep tallow biodiesels. It demonstrates that the fuel properties of biomixtures such as cetane number, viscosity, iodine value, and degree of unsaturation are optimised, resulting in improved combustion characteristics and exhaust gas emissions compared to neat biodiesels. Further studies could be conducted to investigate the effects of different waste biodiesel sources including WCO with an increasing degree of unsaturation and tallows from other animal sources.

Data availability statement

The original contributions presented in the study are included in the article/supplementary material; further inquiries can be directed to the corresponding author.

Author contributions

KM: conceptualization, investigation, methodology, software, validation, visualization, data curation, formal analysis, and writing–original draft. AH: conceptualization, data curation, funding acquisition, investigation, methodology, project administration, resources, software, supervision, validation, visualization, and writing–review and editing. GG: conceptualization, data curation, funding acquisition, methodology, resources, supervision, validation, visualization, and writing–review and editing.

Funding

The authors declare that financial support was received for the research, authorship, and/or publication of this article. This work was partly funded by a DST-UKIERI project. The equipment support provided by the HORIBA United Kingdom company and the help of Salman Safdar are gratefully acknowledged.

Conflict of interest

The authors declare that the research was conducted in the absence of any commercial or financial relationships that could be construed as a potential conflict of interest.

The authors declared that they were an editorial board member of Frontiers at the time of submission. This had no impact on the peer review process and the final decision.

Generative AI statement

The authors declare that no generative AI was used in the creation of this manuscript.

Publisher's note

References

Attia, A. M. A., Nour, M., El-Seesy, A. I., and Nada, S. A. (2020). The effect of castor oil methyl ester blending ratio on the environmental and the combustion characteristics of diesel engine under standard testing conditions. *Sustain. Energy Technol. Assessments* 42, 100843. doi:10.1016/j.seta.2020.100843

Awad, S., Loubar, K., and Tazerout, M. (2014). Experimental investigation on the combustion, performance and pollutant emissions of biodiesel from animal fat residues on a direct injection diesel engine. *Energy* 69, 826–836. doi:10.1016/j.energy.2014.03.078

Bhatti, H. N., Hanif, M. A., Qasim, M., and Ataurrehman, (2008). Biodiesel production from waste tallow. *Fuel* 87, 2961–2966. doi:10.1016/j.fuel.2008.04.016

Borillo, G. C., Tadano, Y. S., Godoi, A. F. L., Pauliquevis, T., Sarmiento, H., Rempel, D., et al. (2018). Polycyclic Aromatic Hydrocarbons (PAHs) and nitrated analogs associated to particulate matter emission from a Euro V-SCR engine fuelled with diesel/biodiesel blends. *Sci. Total Environ.* 644, 675–682. doi:10.1016/j.scitotenv.2018.07.007

Bowden, C. M., Samaga, B. S., and Lyn, W. (1969). Rate of heat release in high-speed indirect injection diesel engines. *Proc. Institution Mech. Eng. Conf. Proc.* 184, 122–129. doi:10.1243/PIME_CONF_1969_184_326_02

British Standard Institution (2010). *Bs En 14214:2008+a1:2009 Automotive fuels — fatty acid methyl esters (FAME) for diesel engines — requirements and test methods*. British Standard Institution., 22. ISBN 978 0 580 70781 0.

Demirbas, A. (2009). Biodiesel from waste cooking oil via base-catalytic and supercritical methanol transesterification. *Energy Convers. Manag.* 50, 923–927. doi:10.1016/j.enconman.2008.12.023

Dhamodaran, G., Krishnan, R., Pochareddy, Y. K., Pyarelal, H. M., Sivasubramanian, H., and Ganeshram, A. K. (2017). A comparative study of combustion, emission, and performance characteristics of rice-bran-neem-and cottonseed-oil biodiesels with varying degree of unsaturation. *Fuel* 187, 296–305. doi:10.1016/j.fuel.2016.09.062

Emiroğlu, A. O., Keskin, A., and Şen, M. (2018). Experimental investigation of the effects of Turkey rendering fat biodiesel on combustion, performance and exhaust emissions of a diesel engine. *Fuel* 216, 266–273. doi:10.1016/j.fuel.2017.12.026

Esso (2019). *Esso synergy diesels*.

European Standard (2009). *European standard EN 590:2013, automotive fuels - diesel - requirements and test methods*, 1–12.

Forte, A., Zucaro, A., Faugno, S., Basosi, R., and Fierro, A. (2018). Carbon footprint and fossil energy consumption of bio-ethanol fuel production from Arundo donax L. crops on marginal lands of Southern Italy. *Energy* 150, 222–235. doi:10.1016/j.energy.2018.02.030

Hajjari, M., Tabatabaei, M., Aghbashlo, M., and Ghanavati, H. (2017). A review on the prospects of sustainable biodiesel production: a global scenario with an emphasis on waste-oil biodiesel utilization. *Renew. Sustain. Energy Rev.* 72, 445–464. doi:10.1016/j.rser.2017.01.034

IEA (2019). *Renewables 2019*. IEA.

Krishna, M. M., Prakash, T. O., Ushasri, P., Janardhan, N., and Murthy, P. V. K. (2016). Experimental investigations on direct injection diesel engine with ceramic coated combustion chamber with carbureted alcohols and crude jatropha oil. *Renew. Sustain. Energy Rev.* 53, 606–628. doi:10.1016/j.rser.2015.09.011

Kumar, A., and Subramanian, K. A. (2017). Control of greenhouse gas emissions (CO2, CH4and N2O) of a biodiesel (B100) fueled automotive diesel engine using increased compression ratio. *Appl. Therm. Eng.* 127, 95–105. doi:10.1016/j.applthermaleng.2017.08.015

Kumar, N., Koul, R., and Singh, R. C. (2022). Comparative analysis of ternary blends of renewable Diesel, diesel and ethanol with diesel. *Sustain. Energy Technol. Assessments* 50, 101828. doi:10.1016/j.seta.2021.101828

Masera, K. (2019). *Biodiesel-biodiesel mixtures to upgrade fuel properties and lower exhaust gas emissions*. Aston University. PhD thesis.

Masera, K., and Hossain, A. K. (2017). Production, characterisation and assessment of biomixture fuels for compression ignition engine application. *Int. J. Mech. Mechatronics Eng.* 11, 1857–1863.

Masera, K., and Hossain, A. K. (2019). Combustion characteristics of cottonseed biodiesel and chicken fat biodiesel mixture in a multi-cylinder compression ignition engine. *SAE Tech. Pap. Ser.* 1, 1–14. doi:10.4271/2019-01-0015

Masera, K., Hossain, A. K., Davies, P. A., and Doudin, K. (2021). Investigation of 2-butoxyethanol as biodiesel additive on fuel property and combustion characteristics of two neat biodiesels. *Renew. Energy* 164, 285–297. doi:10.1016/j.renene.2020.09.064

National Center for Biotechnology Information (2018). *Methyl-alcohol, national center for Biotechnology information, PubChem open chemistry database*.

Özener, O., Yüksek, L., Ergenç, A. T., and Özkan, M. (2014). Effects of soybean biodiesel on a DI diesel engine performance, emission and combustion characteristics. *Fuel* 115, 875–883. doi:10.1016/j.fuel.2012.10.081

Ragit, S. S., Mohapatra, S. K., and Kundu, K. (2010). Performance and emission evaluation of a diesel engine fueled with methyl ester of neem oil and filtered neem oil. *J. Sci. Industrial Res.* 69, 62–66.

Rajamohan, S., Hari Gopal, A., Muralidharan, K. R., Huang, Z., Paramasivam, B., Ayyasamy, T., et al. (2022). Evaluation of oxidation stability and engine behaviors operated by Prosopis juliflora biodiesel/diesel fuel blends with presence of synthetic antioxidant. *Sustain. Energy Technol. Assessments* 52, 102086. doi:10.1016/j.seta.2022.102086

Rajkumar, S., and Thangaraja, J. (2019). Effect of biodiesel, biodiesel binary blends, hydrogenated biodiesel and injection parameters on NOx and soot emissions in a turbocharged diesel engine. *Fuel* 240, 101–118. doi:10.1016/j.fuel.2018.11.141

Ramírez-Verduzco, L. F., Rodríguez-Rodríguez, J. E., and Jaramillo-Jacob, A. D. R. (2012). Predicting cetane number, kinematic viscosity, density and higher heating value of biodiesel from its fatty acid methyl ester composition. *Fuel* 91, 102–111. doi:10.1016/j.fuel.2011.06.070

Refaat, A. A. (2009). Correlation between the chemical structure of biodiesel and its physical properties. *Int. J. Environ. Sci. and Technol.* 6, 677–694. doi:10.1007/BF03326109

Salamanca, M., Mondragon, F., Agudelo, J. R., Benjumea, P., and Santamaria, A. (2012). Variations in the chemical composition and morphology of soot induced by the unsaturation degree of biodiesel and a biodiesel blend. *Combust. Flame* 159, 1100–1108. doi:10.1016/j.combustflame.2011.10.011

Sanjid, A., Kalam, M. A., Masjuki, H. H., Varman, M., Zulkifli, N. W. B. M., and Abedin, M. J. (2016). Performance and emission of multi-cylinder diesel engine using biodiesel blends obtained from mixed inedible feedstocks. *J. Clean. Prod.* 112, 4114–4122. doi:10.1016/j.jclepro.2015.07.154

Sathyamurthy, R., Balaji, D., Gorjian, S., Muthiya, S. J., Bharathwaaj, R., Vasanthaseelan, S., et al. (2021). Performance, combustion and emission characteristics of a DI-CI diesel engine fueled with corn oil methyl ester biodiesel blends. *Sustain. Energy Technol. Assessments* 43, 100981. doi:10.1016/j.seta.2020.100981

Schönborn, A., Ladommatos, N., Williams, J., Allan, R., and Rogerson, J. (2009). The influence of molecular structure of fatty acid monoalkyl esters on diesel combustion. *Combust. Flame* 156, 1396–1412. doi:10.1016/j.combustflame.2009.03.011

Sharma, V., and Ganesh, D. (2019). Combustion and emission characteristics of reformulated biodiesel fuel in a single-cylinder compression ignition engine. *Int. J. Environ. Sci. Technol.* 17, 243–252. doi:10.1007/s13762-019-02285-8

The World Bank (2017). *Fossil fuel energy consumption*.

Tong, D., Hu, C., Jiang, K., and Li, Y. (2011). Cetane number prediction of biodiesel from the composition of the fatty acid methyl esters. *J. Am. Oil Chemists' Soc.* 88, 415–423. doi:10.1007/s11746-010-1672-0

Usta, N., Öztürk, E., Can, Ö., Conkur, E. S., Nas, S., Çon, A. H., et al. (2005). Combustion of bioDiesel fuel produced from hazelnut soapstock/waste sunflower oil mixture in a Diesel engine. *Energy Convers. Manag.* 46, 741–755. doi:10.1016/j.enconman.2004.05.001

Verma, T. N., Nashine, P., Chaurasiya, P. K., Rajak, U., Afzal, A., Kumar, S., et al. (2020). The effect of ethanol-methanol-diesel-microalgae blends on performance, combustion and emissions of a direct injection diesel engine. *Sustain. Energy Technol. Assessments* 42, 100851. doi:10.1016/j.seta.2020.100851

Wakode, V. R., and Kanase-Patil, A. B. (2017). Regression analysis and optimization of diesel engine performance for change in fuel injection pressure and compression ratio. *Appl. Therm. Eng.* 113, 322–333. doi:10.1016/j.applthermaleng.2016.10.178